Measurements of the Inverse Faraday Effect from Relativistic Laser Interactions with an Underdense Plasma

Z. Najmudin,[1] M. Tatarakis,[1] A. Pukhov,[2] E. L. Clark,[1] R. J. Clarke,[3] A. E. Dangor,[1] J. Faure,[4] V. Malka,[4] D. Neely,[3] M. I. K. Santala,[1] and K. Krushelnick[1]

[1]*Imperial College of Science, Technology & Medicine, Prince Consort Road, London SW7 2BZ, United Kingdom*
[2]*Max-Planck-Institut für Quantenoptik, Hans-Kopfermann-Strasse 1, D-85748 Garching, Germany*
[3]*Rutherford Appleton Laboratory, Chilton, Didcot, Oxon OX11 0QX, United Kingdom*
[4]*Laboratoire pour l'Utilisation des Lasers Intenses, CNRS–CEA, École Polytechnique, Palaiseau, France*

(Received 16 October 2000; published 5 November 2001)

Magnetic fields in excess of 7 MG have been measured with high spatial and temporal precision during interactions of a circularly polarized laser pulse with an underdense helium plasma at intensities up to 1×10^{19} W cm^{-2}. The fields, while of the form expected from the inverse Faraday effect for a cold plasma, are much larger than expected, and have a duration approaching that of the high intensity laser pulse (<3 psec). These observations can be explained by particle-in-cell simulations in 3D. The simulations show that the magnetic field is generated by fast electrons which spiral around the axis of the channel created by the laser field.

DOI: 10.1103/PhysRevLett.87.215004 PACS numbers: 52.38.–r, 52.70.Nc, 52.75.Di

Advances in high power laser technology have been rapid over the past few years and presently, tabletop laser systems can routinely produce pulses having a power of many terawatts [1]. For applications such as particle acceleration [2,3], x-ray generation [4], and inertial confinement fusion [5], remarkable progress has been made. However, much of the fundamental physics of these interactions is not yet fully understood.

The generation of magnetic fields in high intensity laser-produced plasmas has recently been the subject of increasing attention [6]. One particular phenomenon, the inverse Faraday effect (IFE), has been a source of some controversy as theoretical predictions are in disagreement [7–9]. IFE is a magneto-optical phenomenon in which the propagation of circularly polarized radiation through a nonlinear medium induces an axial magnetic field along the direction of propagation, due to the transfer of angular momentum from the wave to the medium (in this case to the plasma electrons) [10]. The measurement of relatively small fields generated in this way was reported at low powers in early experiments [11] and recent measurements at intensities of up to 10^{16} W cm^{-2} have shown significant disagreement with theory [12]. For 1 μm wavelength laser radiation at $I = 10^{19}$ W cm^{-2} and a plasma density of 5×10^{19} cm^{-3} calculations [8] predict a magnetic field of greater than 1 MG, which should be localized in space to the focal region of the intense laser pulse. An approximate expression for these fields in uniform plasma is given by [8]

$$B_{\text{uniform}} = \frac{1}{2} B_c \frac{\omega_p^2}{\omega_0^2} \left(\frac{3|a|^2}{2\gamma^2} - \frac{1}{2} \ln \gamma^2 \right), \qquad (1)$$

where B_c is the Compton magnetic field ($m_e c \omega / e$), ω_p is the plasma frequency, ω_0 is the laser frequency, a is the normalized vector potential of the laser field, and γ is the Lorentz factor of the electron laser orbit motion. This expression is modified slightly when the magnetic field is treated self-consistently [8].

This picture is further complicated when an intense laser pulse channels through plasma, so that the electron density is no longer uniform [8,9]. The laser expels cold background electrons out of the channel and the resulting density gradient can result in an additional source of magnetic field, which is comparable in amplitude to that of Eq. (1), but in the opposite direction.

However, the propagation of relativistically intense laser pulses in a plasma is also known to produce axially accelerated electrons [2]. Particle-in-cell (PIC) simulations suggest that these fast electrons are radially confined and perform betatron oscillations in the channel fields [13]. The laser field is found to transfer both linear and angular momentum directly to these resonant particles. In the case of a circularly polarized laser field, the betatron oscillations are spirals around the channel axis and thus the hot electrons can provide an additional source for the axial magnetic field. Using the expression for a simple solenoidal field we can estimate the induced magnetic field as

$$B_{\text{hot}} \approx \alpha B_c \frac{\omega_p}{\omega_0} \frac{n_{\text{hot}}}{n_0} (k_p R), \qquad (2)$$

where α is the average pitch angle of the spiral trajectories of hot electrons, n_{hot} is the density of the hot electrons, R is the channel radius, and $k_p = \omega_p / c$. For electrons in resonance with the laser beam [13], we may set $\alpha = \omega_p / \omega_0$. At relativistic intensities ($a \gg 1$), we estimate the channel radius as $R \sim \pi a / k_p$ and obtain

$$B_{\text{hot}} \approx \pi a B_c \frac{\omega_p^2}{\omega_0^2} \frac{n_{\text{hot}}}{n_0}. \qquad (3)$$

This field may become larger than the fields from (1), as it does not saturate at relativistic intensities and continues to grow with intensity even for $a \gg 1$.

In this paper, we report the first temporally and spatially resolved measurements of Megagauss magnetic fields (up to 7 MG) generated by the hot electron version of IFE in a plasma using a self-channeling laser pulse of relativistic intensity. By comparison with 3D PIC simulations, we show that the observed fields, which exceed the value given by (1), are better explained by Eq. (3).

The experiments were performed using the high intensity VULCAN laser. The laser operates at a wavelength of 1.054 μm and has an energy of up to 40 J per pulse and a pulse duration of between 0.9–1.2 ps. The focal spot was approximately 3 times diffraction limited. In these experiments, the laser pulse was focused into a helium gas jet target using a $f/4$ off-axis parabolic mirror. The "vacuum" intensity was found to reach 1×10^{19} W cm^{-2}. It should be noted that due to self-focusing, it is likely that the actual intensity in localized regions may be higher than this [14]. A $\lambda/4$ wave plate was placed inside the vacuum chamber to change the laser polarization from linear to circular for these measurements.

A small fraction of the pulse was split from the main beam and subsequently frequency doubled to 527 nm for use as a probe beam. The energy of this probe beam was about 100 mJ and the pulse length could be adjusted from 2–15 ps. A fast Hamamatsu streak camera (2–3 ps resolution) was used to measure the duration of the probe beam and to time the probe with the main beam.

Forward Raman scattering was used to determine the plasma electron density. This gave densities consistent with the full ionization of helium neutrals as measured by Moiré deflectometry of the gas jet. It should be noted that no evidence of cavitation (i.e., the depletion of electrons by the ponderomotive force) was observed [15]. The initial plasma electron density could be adjusted systematically throughout the range 4×10^{18}–4×10^{19} cm^{-3}, by changing the backing pressure of the gas jet. Optical probing of the interaction was performed using the same probe beam passing transverse to the direction of propagation of the laser. This gave a measure of the interaction length which was found to be a consistent 1 ± 0.2 mm (about 10 Rayleigh ranges) over this density range, due to self-channeling.

Collinear probing was performed simultaneously with the transverse probing. The collinear probe pulse was linearly polarized and directed onto the same parabolic mirror used to focus the circularly polarized interaction beam into the gas jet. Imaging of the focal plane ensured that the two beams overlapped. Interference filters were used after the interaction, to isolate the collinear probe beam from the main beam. The probe was then imaged onto the slit of the streak camera, which served as the detector. A pair of high extinction ratio polarizers was used to detect Faraday rotation of the probe laser polarization caused by the axial magnetic fields generated by the pump beam in the interaction region [12,16].

Figure 1 presents the typical spatially integrated streak camera signal of the probe beam. Line (*A*) shows the streak when the analyzer is aligned parallel to the probe beam polarization, so that the streak camera captured the unrotated probe light. The duration is 15 ps as expected. The lower line (*B*) shows the signal when the analyzer was crossed with respect to the probe beam polarization. Hence it was set to transmit only light rotated due to the presence of an axial magnetic field. The rotated polarization signal duration was less than 3 ps, which is comparable to the duration of the high intensity laser pulse. In the absence of an axial magnetic field the polarization of the probe radiation would remain unchanged and therefore light would not be transmitted through the analyzer. Shots with only the probe beam showed no rotation, demonstrating that there is no rotation due to the optics. Shots with the plasma generating beam but without probe were taken and only background signal at noise level was observed. Such background shots without probe were taken with the same parameters directly after each data shot, so that this low-level background could be accounted for. As a critical test, when the high intensity interaction beam was linearly polarized, so that no axial magnetic field would be expected, no rotation of the probe polarization was observed. This discounts depolarization due to density gradients within the plasma, and clearly demonstrates that the source of the transmitted signal was the IFE fields generated by the intense circularly polarized laser pulse in the plasma.

With the simultaneous measurement of electron density (from Raman scattering), the magnetic field can be estimated from the intensity ratio between shots with the analyzer crossed and those with the analyzer parallel to the initial polarization of the probe. The peak Faraday rotation angle from Fig. 1 was found to be $22° \pm 3°$ giving a

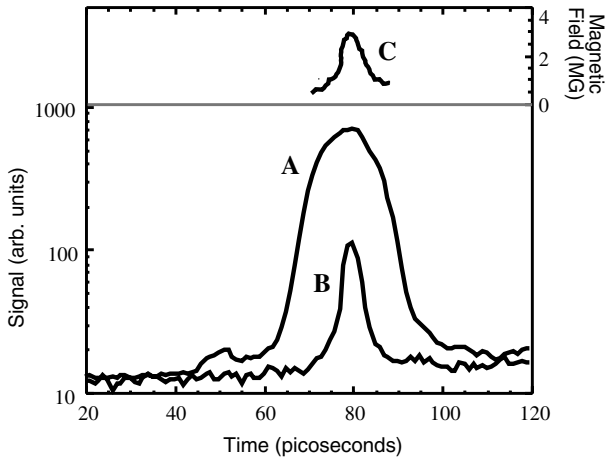

FIG. 1. Streak camera line outs of (*A*) probe pulse — uncrossed analyzer; (*B*) rotated probe — crossed analyzer; (*C*) calculated magnetic field from *A* and *B*.

magnetic field of 2.6 ± 0.6 MG (Fig. 1,*C*) at an electron density of 2.8×10^{19} cm^{-3}. An important aspect of these measurements is that they show that the duration of magnetic fields due to the IFE is approaching that of the intense circularly polarized laser pulse, which generates the field. The dissipation/convection time for such fields is clearly very short—of the order of a picosecond.

In the experiment, we have also imaged the lateral extent of the axial magnetic field in the interaction region. After the interaction region a parabolic mirror relayed the image of the collinear probe in the plasma to a 16-bit CCD array positioned behind a Wollaston prism (analyzer). The prism was set to split the rotated and unrotated parts of the probe beam, so that they could be directly compared. The spatial extent of the rotated beam therefore corresponds to a measurement of the extent of the magnetic field in the plasma, since the spot size of the probe pulse was always much larger than that of the high intensity laser beam. Observations of the radial extent of the magnetic field were made and are shown in Fig. 2, as a function of vacuum-focusable intensity. The peak magnetic field (peak rotation) was always observed on axis, and it was noted that the radial extent of the field decreased as the intensity increased. Similarly, the spatial extent of the high field region decreased at densities which produced the largest magnetic fields. The inset of Fig. 2 shows the magnetic field is localized to 13 ± 2 μm (FWHM) which is significantly smaller than the laser focal spot in vacuum (~20 μm). This is indicative of the self-focusing effects which reduce the region of highest intensity. By rotating the Wollaston prism by 45° to the polarization of the probe beam, the direction of the rotation of the probe polarization, and thus the direction of the magnetic field, could be found. It was found to be consistent with a standard IFE field (i.e., due to a current of electrons rotating in the same direction as the polarization of the laser beam.) This was verified by rotating the quarter wave plate by 90°, which changes the rotation of the laser polarization and also changes the direction of the generated field.

Measurements of the magnetic field strength (spatially integrated, temporal maximum) versus "vacuum" intensity were also made (Fig. 3) for various gas pressures, and it is clear that the field increases with laser intensity. The theoretical expression for a uniform plasma, Eq. (1), with a density of 3.5×10^{19} cm^{-3} is plotted in Fig. 3 for the relativistic regime of our experiments. This expression is easily exceeded by our experimental data. Indeed at lower densities this discrepancy is more than an order of magnitude. The magnetic field due to electron density depletion effect has a similarly small amplitude. It should be noted in Fig. 3 that as the plasma density is increased, the peak measured field did not necessarily increase.

The anomalously high axial magnetic field that we observe in the relativistic regime can be explained by the effect of fast electrons produced during these interactions [Eq. (3)]. In similar experiments arranged so that hot electrons can be detected, we have consistently observed forward accelerated electrons up to 100 MeV in energy (with a "temperature" of up to 10 MeV) [17]. Consequently, we compared our measurements with 3D PIC simulation using the code VLPL [18]. In the simulation, a 30 TW laser beam was incident onto uniform plasma with the density of 3.5×10^{19} cm^{-3}. The laser focal spot radius is 10 μm

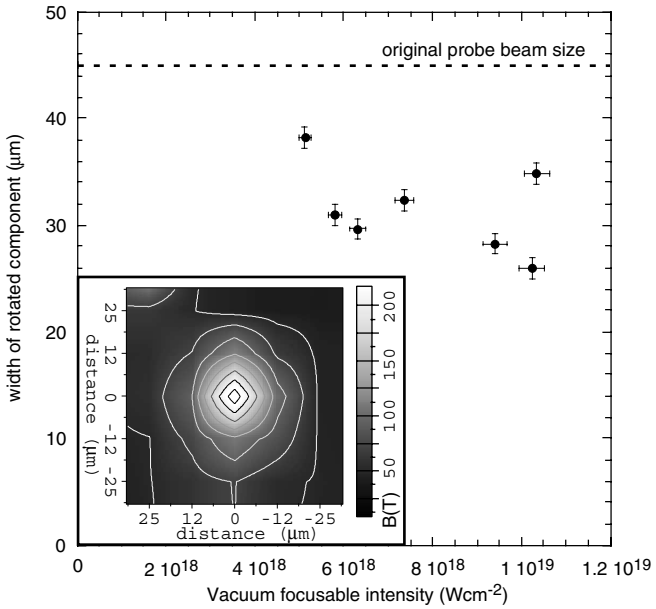

FIG. 2. Spatial extent (FWHM) of B_z as a function of "vacuum" intensity. The extent of the probe beam is marked by dashed line. The inset shows a contour plot of B_z at the focal plane for $I = 6.7 \times 10^{18}$ W cm^{-2}, $n_e = 2.8 \times 10^{19}$ cm^{-3}.

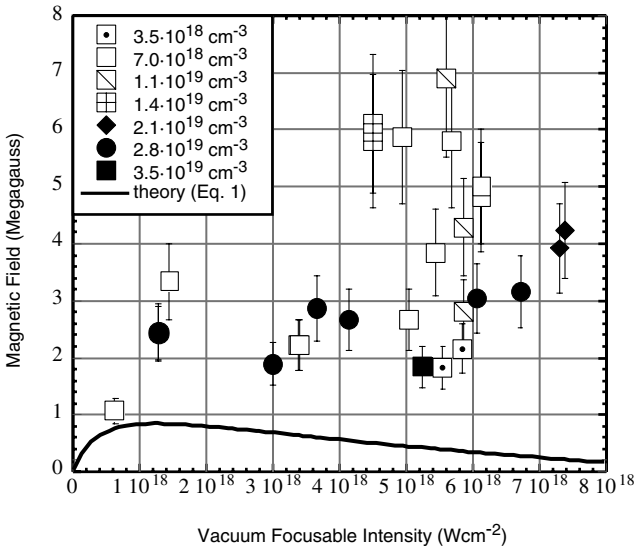

FIG. 3. Measured peak magnetic field versus "vacuum" intensity for various plasma densities (in cm^{-3}). Theoretical curve is from Ref. [8] for $n_e = 3.5 \times 10^{19}$ cm^{-3}.

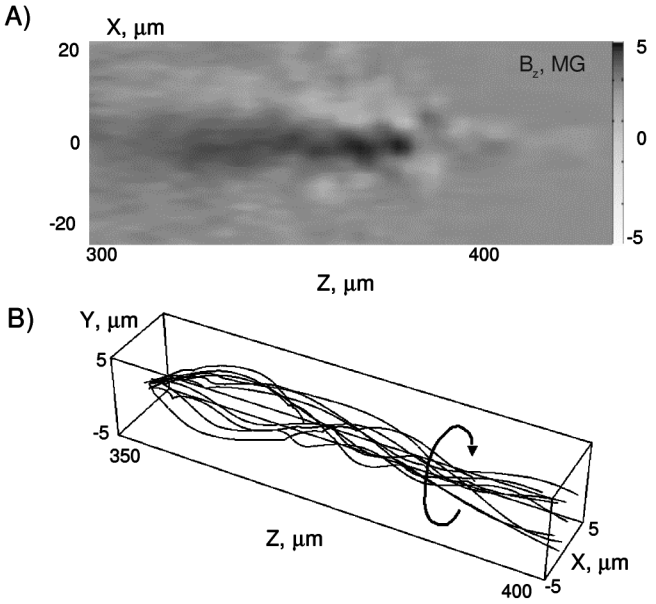

FIG. 4. 3D PIC simulation results. (A) Longitudinal cut of the generated B_z— along the laser beam. The beam has propagated 400 μm through plasma. (B) Trajectories of 10 arbitrarily chosen electrons trapped in the channel. The arrow shows the direction of circulation.

corresponding to an initial intensity of 10^{19} W cm^{-2}. Because of computer limitations, the simulation was run for only a laser pulse duration of 200 fs.

The axial magnetic field obtained in the simulation is shown in Fig. 4(A). The maximum generated field is about 5 MG, significantly higher than Eq. (1) predicts, but in line with the estimate (3). The principal difference concerns the electron trajectories in the laser field. The derivation of Eq. (1) implies that plasma electrons orbit around their initial transverse positions due to the laser field, while (3) is based on the hypothesis that the electrons orbit around the channel axis. These resonantly driven betatron oscillations in the channel fields have much larger spatial extent than the simple electron quiver motion in the laser field. Consequently, higher magnetic fields can be produced. In the PIC simulation, electrons trapped in the channel were followed and trajectories of 10 arbitrary sampled electrons are shown in Fig. 4(B) in a perspective view. Clearly, the electrons are circulating around the channel axis. The characteristic radii of the orbits are 5 μm. This is an order of magnitude more than that due to the quiver motion in the laser field. The large number of energetic electrons required to explain such magnetic fields (greater than 10% of ambient electrons) is consistent with the high electron yields measured in these experiments [17]. The direction of the electron spiraling corresponds, as it should, to the direction of rotation of the laser polarization and to the sign of the observed magnetic field.

In conclusion, we have performed the first time and space-resolved measurements of the inverse Faraday effect, in which we measure peak fields of the order of 7 ± 0.8 MG from interactions at relativistic intensities. The field was generated by a 0.9 psec duration laser pulse and lasted for less than 3 psec. The measured field is much greater than that predicted by recent theoretical predictions for IFE in a cold plasma [7–9]. However, 3D PIC simulations produce magnetic fields of similar amplitude, demonstrating that at these intensities the axial magnetic field can be due to betatron trajectories of the accelerated electrons in the plasma channel produced by the circularly polarized laser. Such magnetic fields have significance for laser plasma accelerator research in reducing plasma propagation instabilities of laser-produced electron beams and perhaps in improving their emittance.

We would like to acknowledge the technical assistance of the VULCAN operations team and useful discussions with G. Shvets and M. G. Haines.

[1] M. Perry and G. Mourou, Science **264**, 917 (1994).
[2] A. Modena *et al.,* Nature (London) **377**, 606 (1995); E. Esarey *et al.,* IEEE Trans. Plasma Sci. **24**, 252 (1996).
[3] E. L. Clark *et al.,* Phys. Rev. Lett. **84**, 670 (2000).
[4] Z. H. Chang *et al.,* Phys. Rev. Lett. **79**, 2967 (1997); C. Spielmann, Science **278**, 661 (1997).
[5] M. Tabak *et al.,* Phys. Plasmas **1**, 1626 (1994).
[6] S. C. Wilks *et al.,* Phys. Rev. Lett. **69**, 1383 (1992); R. J. Mason and M. Tabak, Phys. Rev. Lett. **80**, 524 (1998); A. Pukhov and J. Meyer-ter-Vehn, Phys. Rev. Lett. **76**, 3975 (1996).
[7] V. Y. Bychenkov *et al.,* Sov. Phys. JETP **78**, 62 (1994); A. D. Steiger and C. H. Woods, Phys. Rev. A **5**, 1467 (1972); T. Lehner, Phys. Scr. **49**, 704 (1994).
[8] Z. M. Sheng and J. Meyer-ter-Vehn, Phys. Rev. E **54**, 1833 (1996).
[9] L. M. Gorbunov and R. R. Ramazasvili, JETP **87**, 461 (1998).
[10] M. G. Haines, Phys. Rev. Lett. **87**, 135005 (2001).
[11] J. P. van der Ziel *et al.,* Phys. Rev. Lett. **15**, 190 (1965); J. Deschamps *et al.,* Phys. Rev. Lett. **25**, 1330 (1970).
[12] Y. Horovitz *et al.,* Phys. Rev. Lett. **78**, 1707 (1997); T. Lehner, Europhys. Lett. **50**, 480 (2000).
[13] A. Pukhov *et al.,* Phys. Plasmas **6**, 2847 (1999).
[14] K. Krushelnick *et al.,* Phys. Rev. Lett. **83**, 737 (1999).
[15] K.-C. Tzeng and W. B. Mori, Phys. Rev. Lett. **81**, 104 (1998).
[16] I. H. Hutchinson, *Principles of Plasma Diagnostics* (Cambridge University Press, Cambridge, 1987).
[17] M. I. K. Santala *et al.,* Phys. Rev. Lett. **86**, 1227 (2001).
[18] A. Pukhov, J. Plasma Phys. **61**, 425 (1999).